Thickness-dependent electronic structure in ultrathin $LaNiO_3$ films under tensile strain

Hyang Keun Yoo,[1,2] Seung Ill Hyun,[3] Young Jun Chang,[4,5] Luca Moreschini,[5] Chang Hee Sohn,[1,2] Hyeong-Do Kim,[1,2,*] Aaron Bostwick,[5] Eli Rotenberg,[5] Ji Hoon Shim,[3,6] and Tae Won Noh[1,2]

[1]*Center for Correlated Electron Systems, Institute for Basic Science (IBS), Seoul 151-747, Republic of Korea*

[2]*Department of Physics and Astronomy, Seoul National University, Seoul 151-747, Republic of Korea*

[3]*Department of Chemistry, Pohang University of Science and Technology, Pohang 790-784, Republic of Korea*

[4]*Department of Physics, University of Seoul, Seoul 130-743, Republic of Korea*

[5]*Advanced Light Source, Lawrence Berkeley National Laboratory, Berkeley, California 94720, USA*

[6]*Division of Advanced Nuclear Engineering, Pohang University of Science and Technology, Pohang 790-784, Republic of Korea*

(Received 27 October 2014; revised manuscript received 4 November 2015; published 29 January 2016)

We investigated electronic-structure changes of tensile-strained ultrathin $LaNiO_3$ (LNO) films from ten to one unit cells (UCs) using angle-resolved photoemission spectroscopy (ARPES). We found that there is a critical thickness t_c between four and three UCs below which Ni e_g electrons are confined in two-dimensional space. Furthermore, the Fermi surfaces (FSs) of LNO films below t_c consist of two orthogonal pairs of one-dimensional (1D) straight parallel lines. Such a feature is not accidental as observed in constant-energy surfaces at all binding energies, which is not explained by first-principles calculations or the dynamical mean-field theory. The ARPES spectra also show anomalous spectral behaviors, such as no quasiparticle peak at the Fermi momentum but fast band dispersion comparable to the bare-band one, which is typical in a 1D system. As its possible origin, we propose 1D FS nesting, which also accounts for FS superstructures observed in ARPES.

DOI: 10.1103/PhysRevB.93.035141

I. INTRODUCTION

Dimensionality and strain control are at the heart of ultrathin-film engineering [1–8]. As the film thickness t approaches one unit cell (UC), quantum confinement restricts electronic motion within a two-dimensional (2D) plane [5–7]. In a strongly correlated transition-metal oxide (TMO), such 2D confinement is crucial in determining its electronic properties due to the balance between electronic kinetic motion and correlation [9]. Thus, the dimensionality can be used as a key parameter to control various physical properties of TMOs. Additionally, because quantum correlation becomes strong in lower dimensions, it can drive a TMO film to reach a novel quantum phase [10,11]. In recent decades, many studies have been devoted along this direction to search for new interesting phenomena [3,5–8]. However, fundamental understandings on the phenomena appearing in ultrathin TMO films remain challenging [5–7]. This is due, in part, to the difficulty in preparing high-quality ultrathin films and measuring their electronic structures *in situ* by state-of-the-art spectroscopy techniques, such as angle-resolved photoemission spectroscopy (ARPES).

Among numerous TMOs, $LaNiO_3$ (LNO) has recently attracted much interest, partly due to its potential electronic analog to high-T_c cuprate superconductors under the conditions of tensile strain and reduced dimensionality [12–14]. Although superconductivity in nickelates has not yet been realized and theoretical controversy has been provoked [15,16], other interesting results have been reported upon reducing its dimensionality. Among them, observation of a metal-insulator transition (MIT) [17–19] and a spin/charge ordering [20–22] below a critical thickness t_c have drawn much attention. These phenomena were proposed to originate from novel electronic phases attained by changing the dimensionality. Direct observations of their electronic structures followed, but the results are controversial. Using soft x-ray photoemission spectroscopy, Sakai *et al.* [23] observed "gradual" localization of Ni 3*d* electrons in "compressively strained" ultrathin LNO films on a $LaAlO_3$ substrate. In contrast, King *et al.* [24], by ARPES using He I and II radiation, reported "abrupt" destruction of Fermi-liquid-like quasiparticles on a similar LNO film, which was attributed to a fluctuating spin order enhanced by quantum confinement.

Here, we investigate the electronic structures of "tensile-strained" ultrathin LNO films using *in situ* ARPES utilizing synchrotron radiation. By reducing the LNO film thickness consecutively from ten to one UCs, we found abrupt changes in the electronic structures at a critical thickness t_c, consistent with earlier resistivity measurements [20,21]. However, the Fermi-surface (FS) topology is quite different from that of high-T_c cuprate superconductors, and the ARPES spectra unexpectedly show finite spectral weight at the Fermi level (E_F) even in the insulating phase. Furthermore, below t_c's between three and four UCs, e_g electrons behave as if they are not only confined on a 2D plane, but also moving along a one-dimensional (1D) line. Such a 1D characteristic cannot be easily derived from an e_g-orbital manifold. We suggest that this bizarre behavior could be explained by 1D FS nesting. Thus, ultrathin LNO films provide an intriguing platform to investigate anomalous properties in strongly correlated TMO films.

II. METHODS

High-quality epitaxial $LaNiO_3/LaAlO_3/Nb:SrTiO_3$ films were fabricated using pulsed laser deposition (PLD). We used a KrF excimer laser ($\lambda = 248$ nm) with a repetition rate of 2 Hz to ablate sintered stoichiometric targets. The laser energy density was $1-1.5\,J\,cm^{-2}$ at the target position. Before PLD, atomically flat 0.5-wt %-Nb-doped $SrTiO_3$ (STO) substrates

*hdkim6612@snu.ac.kr

were prepared using buffered hydrofluoric acid etching and heating processes. The STO substrates were conducting due to Nb doping, which prevented charging problems during the ARPES measurements. Additionally, to avoid possible intermixing between La and Sr, we deposited a 15-UC-thick $LaAlO_3$ buffer layer. Finally, we deposited one to ten UCs of LNO films by monitoring the film thickness with *in situ* reflection high-energy electron diffraction. To prevent quality variation among films, we deposited all of the films between one and ten UCs at once by selectively choosing the deposited area using a mechanical shutter, called a "staircase structure." We confirmed that a 30-UC-thick LNO film grown on STO under the same deposition conditions was fully and homogeneously strained (tensile misfit strain of +1.7%) using synchrotron-based x-ray diffraction at the 9C Beamline of the Pohang Light Source. Therefore, all of the ultrathin LNO films used in this study should have been fully strained under a tensile misfit strain.

All measurements were performed at an end station equipped with ARPES and PLD at the Beamline 7.0.1 of the Advanced Light Source. After deposition, the thin films were transferred without breaking a vacuum to an analysis chamber with a base pressure of 5×10^{-11} Torr. The sample temperature was kept at 90 K, except for the cases specified. The total-energy resolution was about 30 meV at $h\nu = 150$ eV. ARPES measurements were carried out on the ΓXM and the *ZRA* symmetry planes at $h\nu = 157$ and 120 eV, respectively, which were determined by varying the photon energy at normal emission.

III. RESULTS AND DISCUSSION

A. Abrupt electronic-structure change by dimensionality control

We investigated how the electronic structure of a tensile-strained LNO film evolves with thicknesses ranging from ten to one UCs by ARPES. Because we are dealing with ultrathin films, it may be plausible to use surface Brillouin-zone notation. However, our ten-UC LNO film exhibits a three-dimensional (3D) electronic structure with electron and hole pockets located at the Γ and A points, respectively [25]. These are consistent with band-calculation results for bulk LNO [26] and the results from an earlier soft x-ray ARPES study [27] on a much thicker (about 50-UC) film. Thus, for convenience, we use the notation for a bulk tetragonal structure.

Figure 1 shows the thickness-dependent electronic structures of LNO films measured by ARPES. As the thickness decreased down to four UCs, we can see some gradual changes, but their spectral features remain essentially the same. Note that ARPES measures only the topmost several layers due to short photoelectron escape depth. Additionally, the thickness of a thin-film thickness may not be so uniform over the measured area. This may explain the gradual localization in the experimental ARPES spectra in Ref. [23] in which the photoelectron escape depth was somewhat larger than those of other ARPES measurements [24], including ours.

However, another one-UC reduction from the UCs results in dramatic electronic-structure changes as follows. (1) FSs on the ΓXM and the *ZRA* planes become nearly identical as shown in Figs. 1(d)–1(f). (2) The band dispersions along the ΓXM and the *ZRA* lines are also nearly the same [Figs. 1(j)–1(l)]. (3) Strongly renormalized quasiparticle peaks along the ΓXM and the *ZRA* lines in thick films disappear. Instead, a faint but fast band appears. (4) The size of the electron pocket at the Γ point becomes smaller but does not vanish. The MDC plots in Supplemental Material (SM) Fig. S2 show more clearly that these abrupt electronic-structure changes take place at t_c's between four and three UCs [28].

The observations (1) and (2) imply that the k_z dependence in the electronic structure disappears, indicating that the 3D electronic structures in the thick ($t > t_c$) films become 2D-like ones at $t < t_c$. The critical thickness value is consistent with our resistance measurements (SM Fig. S4) that show a MIT at t_c. Thus, we conclude that there is an abrupt electronic phase transition at t_c. Our critical-thickness value is one UC larger than that reported in a previous ARPES study [24]. However, the overall features of the spectral changes are similar. The difference may originate from a reduced strain in our study. Note that our results are consistent with other resistivity measurements using $SrTiO_3$ substrates [20,21].

B. Electronic analog to high-T_c cuprates?

Even though bulk LNO is a simple paramagnetic metal at all temperatures [29], it has attracted much attention because of its potential to be an electronic analog to high-T_c cuprate superconductors via strain and dimensionality control [12–14]. Now, our LNO films below t_c will be a good test bed for this theoretical proposal because it is under 1.7% tensile strain and well confined in 2D. According to the observation (4) in the previous section, the electron pocket at the Γ point does not vanish even at one UC although its volume gradually decreases. Thus, we can conclude that the high-T_c cupratelike electronic structure in ultrathin LNO films is difficult to achieve at least under these conditions. We can think of hole doping for this end to push away the electron pocket, but it will be a more difficult task because a formally Ni^{4+} or O^{1-} ion is chemically unfavorable.

The original proposal is based on the effective two-band Hubbard model solved by the dynamical mean-field theory (DMFT) [13,14]. The single-band physics as in cuprates [30] could be achieved by large crystal-field splitting and quantum confinement. However, if the O $2p$ degrees of freedom are explicitly taken into account, then the orbital polarization is not so considerable as in the two-band model, and the FS topology does not change [15]. Such behavior was examined by thorough comparison of both models and attributed to Hund's coupling between two d electrons that plays an important role when about one electron is transferred from the O $2p$ orbitals [16]. Our ARPES results strongly suggest that the charge-transfer energy in LNO is so small or negative that the O $2p$ degrees of freedom cannot be integrated out.

C. Anomalous electronic structure below t_c

As shown in Figs. 1(d)–1(f), FSs in LNO films below t_c are composed of pairs of parallel straight lines along the k_x and k_y axes. These parallel lines on the $k_x - k_y$ plane are the

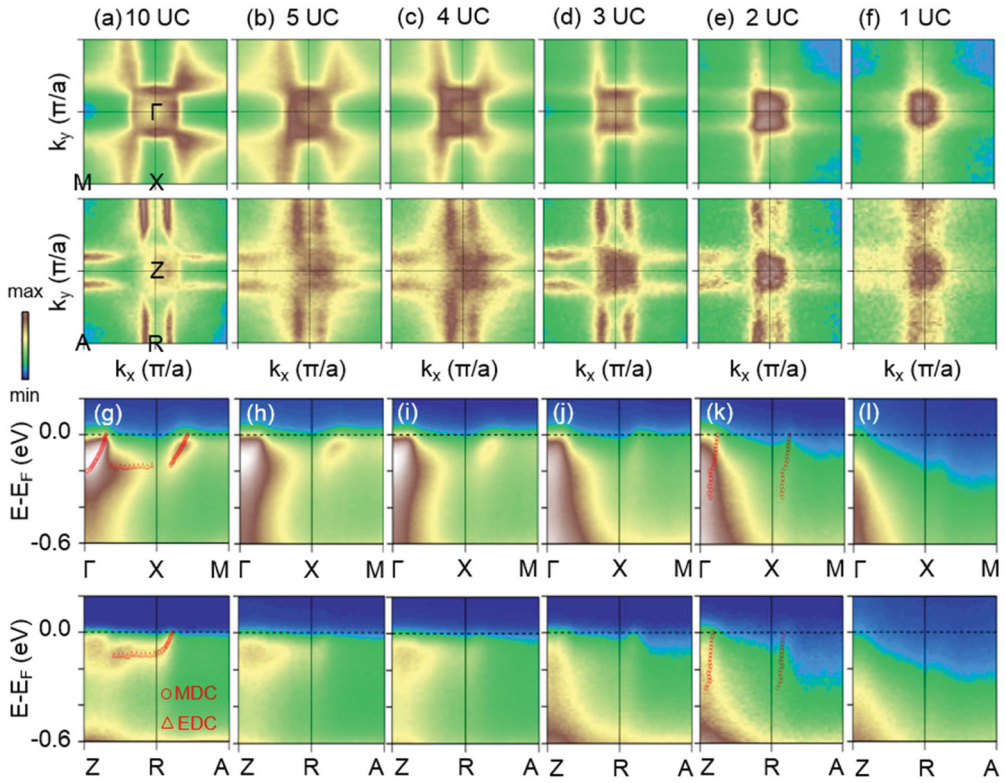

FIG. 1. (a)–(f) FSs in the Γ*XM* (upper panel) and the *ZRA* (lower panel) planes of tensile-strained LNO films from ten to one UCs obtained by ARPES. As the thickness changes from four to three UCs, we can see an abrupt fermiology change, i.e., the FSs on both symmetry planes become nearly identical and consist of two parallel straight lines along the k_x and the k_y axes. (g)–(l) ARPES images along the Γ*XM* (upper panel) and the *ZRA* (lower panel) lines. To show the changes in band dispersions by thickness control more clearly, the relative intensity maxima in momentum distribution curves (MDCs) or energy distribution curves (EDCs) are plotted with empty circles and triangles, respectively, in (g) and (k). As the thickness is reduced from four to three UCs, the band dispersions change dramatically from those of the ten-UC film. Additionally, they become nearly identical along the Γ*XM* and the *ZRA* lines. Thus, a critical thickness t_c between four and three UCs is identified at which the electronic structures of the LNO films under tensile strain qualitatively show a different nature.

signature of quasi-1D nature in the electronic structure [31,32]. Additionally, the essentially identical band dispersions along the *X*Γ*X* and the *MXM* lines for $t < t_c$ [Fig. 2(a)] provide further compelling evidence for the quasi-1D nature. In contrast, Fig. 2(b) shows different band dispersions along the same symmetry lines for the ten-UC film. The band calculations using the GGA for the one-UC LNO show that the band along the *X*Γ*X* line has a strong $3z^2-r^2$ character, whereas the band along the *MXM* line has a heavily mixed orbital character of $3z^2-r^2$ and x^2-y^2 as shown in Fig. 2(e). Thus, the dispersion along the *MXM* line for $t > t_c$ should be much faster than that along the *X*Γ*X* line as shown in Fig. 2(b). Despite different orbital characters, the nearly same band dispersions in Fig. 2(a) suggest that there should be some underlying mechanism for such unexpected behavior.

To determine whether or not the band dispersions are truly 1D-like over the entire energy-momentum space, CES maps for the two-UC film are depicted in Figs. 2(c) (Γ*XM* plane) and 2(d) (*ZRA* plane) down to −0.4 eV in increments of −0.1 eV. If the quasi-1D-like fermiology is accidental, then the CES maps at deeper binding energies should show a dispersive 2D shape on the k_x-k_y plane. Quite surprisingly, the pair of two parallel straight lines is well preserved at all binding energies with only broadening and a slight reduction in the distance between them. These results strongly suggest that the abrupt change in the electronic structure at t_c is related not only to 2D quantum confinement, but also to the quasi-1D behavior.

Figure 2(e) shows CES maps calculated using the GGA for a one-UC LNO. In contrast to the measurements, the 2D nature of the electronic structure is quite evident. To determine whether or not the quasi-1D behavior can be explained by local correlation effects, we performed GGA + DMFT calculations. As depicted in Fig. 2(f), the fermiology is somewhat similar to the ARPES results except for a slight gap between the electron and the hole pockets along the Γ*M* line. However, the CES map at −0.1 eV deviates significantly from the 1D nature. CES maps from the GGA + DMFT calculations at higher binding energies are similar to those shown in Figs. 2(c) and 2(d). However, these features arise from incoherent excitations because the minimum of the quasiparticle dispersion is located at about −0.2 eV (SM Fig. S5). Thus, the 1D-like behavior cannot be explained within the DMFT picture.

D. Anomalous single-hole dynamics

Along with the anomalous behavior in the fermiology and the band dispersions below t_c, we also observed peculiar spectral features in ARPES. Figure 3 compares ARPES

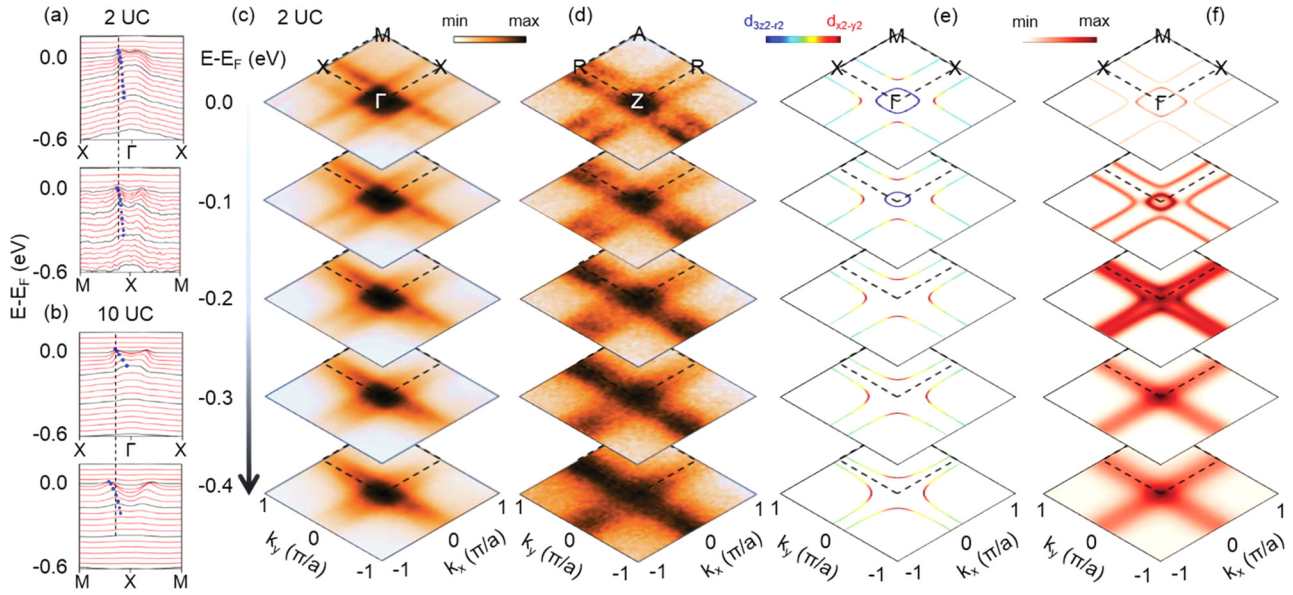

FIG. 2. (a) MDC stack plots of the band dispersions for two UCs along the $X\Gamma X$ (upper panel) and the MXM (lower panel) lines. The blue circles indicate the peak positions in the MDCs. (b) The same as in (a) but for ten UCs. The dashed lines are guidelines for the comparison of the band dispersions along the $X\Gamma X$ and the MXM lines. In two UCs, they are almost identical, whereas they are quite different in ten UCs. Constant-energy-surface (CES) maps for two UCs (c) on the ΓXM and (d) on the ZRA planes at a binding energy ranging from 0 to 0.4 eV. All CES maps show pairs of parallel straight lines along the k_x and the k_y axes, irrespective of binding energy. These results strongly suggest the quasi-1D nature of the electronic structures in the LNO films below t_c. CES maps for one UC (e) from the generalized gradient approximation (GGA) and (f) from the dynamical mean-field theory combined with the GGA (GGA + DMFT). The e_g-orbital contributions are shown by rainbow image scales in (e). The CES maps from the GGA calculations show a clear 2D nature. The fermiology from the GGA + DMFT calculations looks similar to that from the ARPES data; however, a slight increase in the binding energy reveals two-dimensional features. The similar cross shapes of the CESs at higher binding energies ($\geqslant$0.2 eV) originate from incoherent excitations.

spectra along the XM lines for ten and two UCs. In contrast to the ten-UC film in which a strongly renormalized band crosses the E_F [Fig. 3(a)] and quasiparticle peaks are well defined [Fig. 3(b)], the band in the two-UC film exhibits a diffuse feature despite its much faster dispersion [Fig. 3(c)]. Moreover, the ARPES spectral weight at E_F is strongly suppressed below t_c [Fig. 3(d)] as clearly shown by comparing E_F-symmetrized spectra at the Fermi momenta for various thicknesses [Fig. 3(e)]. Such behavior could be understood by 1D-like fermiology because there is no Fermi-liquid quasiparticle in a 1D system [33,34].

We also compare the ARPES band dispersions with the GGA (black solid lines) and the GGA + DMFT (red open circles) calculations in Figs. 3(a) and 3(c) for the ten- and two-UC films, respectively. For the ten-UC film, the GGA + DMFT calculations well describe the dispersion, thus Fermi-liquid behavior is expected in this case. On the other hand, for the two-UC film, the dispersion is surprisingly well fit by the GGA calculations, i.e., the bare-band dispersion, which is opposite from our naive expectation that a quantum correlation should play an important role in low-dimensional systems. Note that this behavior is also reminiscent of the single-hole dynamics in cuprate oxides, which differs considerably depending on its dimensionality [35]. In the 2D cuprate $Sr_2CuCl_2O_2$, for example, ARPES spectra show a very narrow band [36]. However, in a 1D cuprate $SrCuO_2$ in which spin and charge degrees of freedom are well separated, the "holon"-branch dispersion is as fast as that of the bare band [35,37].

E. Fermi-surface nesting and possible one-dimensional spin order

Figure 4(a) shows a FS map for the two-UC LNO film. In our previous study [25], we could observe FS superstructures for compressive and tensile-strained ten-UC LNO films, which were attributed to charge disproportionation and additional spin-density-wave (SDW) fluctuations in three dimensions. A FS superstructure can also be observed in the two-UC film, similar to but much stronger than that in the tensile-strained ten-UC film. In the bulklike ten-UC film, the superstructure may originate from FS nesting with a $\mathbf{Q} = (1/4,1/4,1/4)$ modulation. However, below t_c, the nesting vector should be modified to $\mathbf{Q} = (1/4,1/4,0)$ or $(1/4,0,0)$ due to the lower dimensionality. According to recent calculations by Lee *et al.* [38], as the LNO film thickness decreases, the spin susceptibility along the (100) direction becomes larger than that along the (110) direction. Thus, we can expect 1D nesting, i.e., $\mathbf{Q} = (1/4,0,0)$. Here, we will neglect the possible checkerboard-type charge ordering present in other bulk nickelates [39,40] because it is not relevant to the 1D electronic structure. In addition, note that since we did not observe any significant signature corresponding to surface reconstruction in the electron-diffraction patterns, we may exclude the possibility that surface reconstruction is the origin of the FS superstructure (SM Fig. S1).

If the nesting is strong enough to completely remove the spectral weight at E_F, then the film will have a FS only along one direction. (Note that there will be a twin FS along the

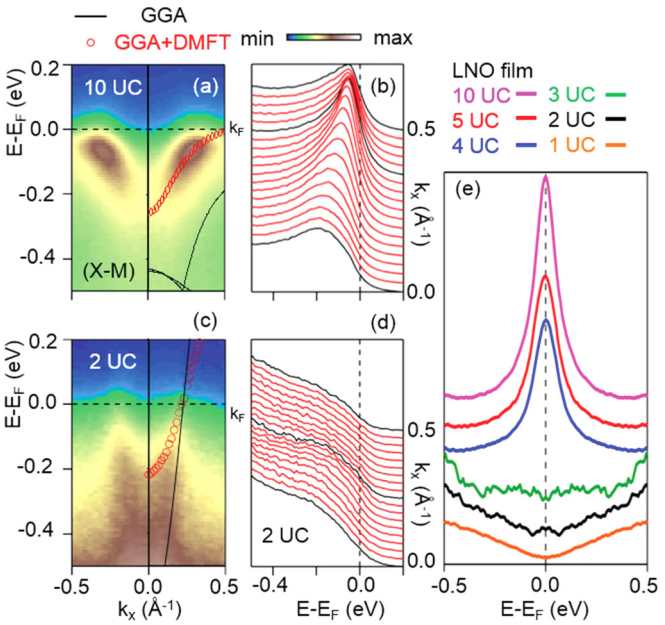

FIG. 3. (a) Band dispersion and (b) EDC stack plot along the *MXM* line for ten UCs. The band structure and a quasiparticle peak at E_F are well defined. (c) and (d) The same as in (a) and (b) but for two UCs. (e) Symmetrized EDC plots with respect to the Fermi level. Below t_c, the band dispersion is much faster but more diffuse than that above t_c. No well-defined quasiparticle peak is observed, and the ARPES spectral weight at the Fermi momentum is strongly suppressed. The black solid lines and the red empty circles represent the dispersion from the GGA and the GGA + DMFT calculations, respectively. For the ten-UC film, the dispersion is well described by the GGA + DMFT calculations with strong electron renormalization. In contrast, for the two-UC film, it is well fit by the GGA calculations.

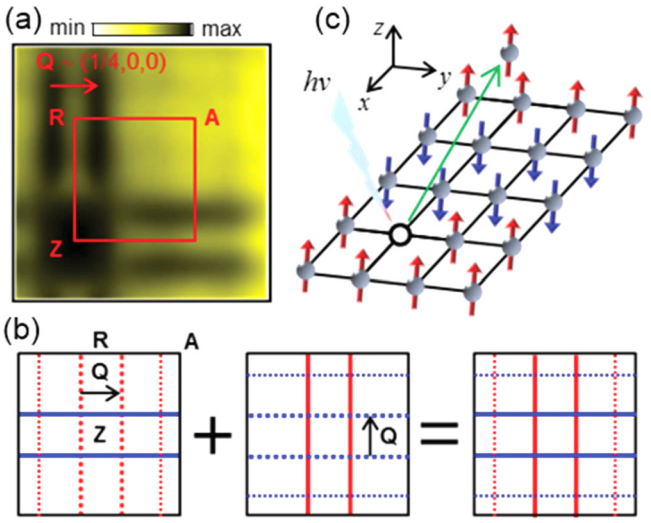

FIG. 4. (a) FS map for three UCs with a nesting vector $\mathbf{Q} \sim (1/4,0,0)$ which shows a corresponding FS superstructure. The map was symmetrized with respect to the mirror planes and plotted using a logarithmic scale. Note that a 90°-rotated domain would equally populate in the film. (b) Schematics of a 1D FS and its superstructure. Because the FS is not fully gapped, it is represented by thick dashed lines, and its superstructure is represented by thin ones. If we consider equivalent domains, then the final FS and its superstructure will correspond to the rightmost one. (c) The schematic 1D spin-ordering model with $\mathbf{Q} = (1/4,0,0)$ to explain the diffuse but fast 1D band dispersion. In this diagram, a hole produced in an ARPES process is free to hop along the y axis, but it costs significant energy to move along the x axis due to spin-order breaking.

perpendicular direction because we can expect that a 90°-rotated domain will populate equally.) However, the existence of the FS superstructure implies that the gap does not fully open. In Fig. 4(b), we depicted schematics of the FS and its superstructure due to 1D nesting with $\mathbf{Q} = (1/4,0,0)$. The left diagram demonstrates that there is FS nesting along the k_x direction, transferring some spectral weight at E_F (represented by thick dashed lines) to the FS superstructure (represented by thin dashed lines), whereas the 1D FS along the k_y direction remains unchanged (represented by solid lines). In the middle diagram, the twin FS and its superstructure are shown as noted above. As a result, the FS map will be given as in the right diagram, in good agreement with the experimental FS map shown in Fig. 4(a).

In Fig. 4(c), a possible spin ordering due to the 1D FS nesting is schematically depicted. The nesting vector $\mathbf{Q} = (1/4,0,0)$ will stabilize a SDW state in which the spins are antiferromagnetically aligned along the x axis with an "up-up-down-down" spin pattern, whereas it has a ferromagnetic order along the y axis [38]. If we remove an electron from this state via an ARPES process, the resulting single hole will have different dynamics depending on its direction of motion. Hole hopping along the x axis costs considerable energy to break the spin-ordering pattern. Thus, the spectral weight around E_F should be transferred to a higher binding energy. On the other hand, when the hole hops along the y axis, its motion is rather free, making a fast band similar to that from the GGA calculations. As a result, the hole motion becomes quasi-1D. But, as is well known, Fermi-liquid quasiparticles do not exist in quasi-1D systems [41–43], thus the spectral weight near E_F is strongly suppressed, and the bands are quite diffuse. Note that according to the picture in Fig. 4(c), no spin excitation occurs when the hole moves along the y axis. Therefore, there should be no well-separated "spinon" branch, which is consistent with our ARPES spectra shown in Fig. 3(c). Similar behavior was also observed in a recent ARPES study of a quasi-1D Mo blue bronze where spinon and holon branches are smeared into an unexpectedly broad single band [43]. In short, the single ansatz of 1D FS nesting, which leads to 1D SDW formation, the anomalous spectral features, i.e., the 1D-like fast band dispersion and the spectral-weight suppression near the E_F below t_c can be described. To confirm this picture, structural studies, such as spin-polarized scanning tunneling microscopy [44] and resonant soft x-ray scattering [22], are immediately suggested.

F. Metal-insulator transition associated with dimensional crossover

Although our ARPES spectra show that a Luttinger FS persists down to the one-UC film, numerous studies have reported the insulating properties of such ultrathin LNO films and superlattices [17–24]. To explain the insulating ground state, several mechanisms have been proposed, such as charge disproportionation [20] and Mott transition due to band

narrowing by quantum confinement [21]. Our *ex situ* transport measurements also showed an insulating temperature dependence below t_c (SM Fig. S4). However, we can rule out these two possibilities because they should have a full gap. Another possibility is that the insulating behavior originates from the generation of a large percolating cluster of insulating channels in ultrathin films [8]. *In situ* local probe measurements, such as conducting atomic force microscopy and scanning tunneling microscopy, could be the most effective method to investigate the percolating phenomena. However, such measurements remain challenging with oxide heterostructures. Instead, we observed nearly temperature-independent ARPES data of the three-UC-thick LNO film (SM Fig. S3). If there are significant percolating channels, we might be able to observe a temperature-dependent change in the photoemission spectra due to phase separation [45]. This result suggests, therefore, that percolating channels might be not the origin of the insulating behavior in our ultrathin films.

Disorder effects, such as Anderson localization, play an important role in low-dimensional systems, especially with regard to their transport properties. It is well known that any slight disorder in low dimensions can cause insulating behavior [46,47]. This is consistent with earlier transport studies that emphasize the role of Anderson localization for insulating states [17,18]. However, the localization cannot clearly explain the electronic-structure changes shown in this paper; the quasi-1D nature of the electronic structure due to 1D FS nesting remains the dominant factor governing the single-hole dynamics.

IV. CONCLUSION

In conclusion, we directly investigated the change in the electronic structure of ultrathin LNO films by dimensionality control, combining an *in situ* APRES system with state-of-the-art film fabrication. We found anomalous electronic-structure changes in ultrathin films below t_c. The GGA + DMFT calculations show that consideration of the local correlation cannot account for such changes. As a possible origin, we propose the 1D FS nesting to explain the FS superstructure as well as the anomalous electronic structure. Further experimental and theoretical works are necessary to clarify its origin.

ACKNOWLEDGMENTS

The authors are grateful to H. W. Park and S. B. Lee for useful discussions. This work was supported by Grant No. IBS-R009-D1. J.H.S. was supported by the Nano-Material Technology Development Program (Green Nano Technology Development Program) through the National Research Foundation of Korea (NRF) funded by the Ministry of Education, Science and Technology (Grant No. 2011-0030146). L.M. acknowledges support by a grant from the Swiss National Science Foundation (SNSF) (Project No. PA00P21-36420). Y.J.C. acknowledges support from National Research Foundation of Korea under Grant No. NRF-2014R1A1A1002868. The Advanced Light Source is supported by the Director, Office of Science, Office of Basic Energy Sciences of the U.S. Department of Energy under Contract No. DE-AC02-05CH11231.

[1] S. Ghosh, W. Bao, D. L. Nika, S. Subrina, E. P. Pokatilov, C. N. Lau, and A. A. Balandin, Nature Mater. **9**, 555 (2010).
[2] Y. Zhang, K. He, C.-Z. Chang, C.-L. Song, L.-L. Wang, X. Chen, J.-F. Jia, Z. Fang, X. Dai, W.-Y. Shan, S.-Q. Shen, Q. Niu, X.-L. Qi, S.-C. Zhang, X.-C. Ma, and Q.-K. Xue, Nat. Phys. **6**, 584 (2010).
[3] J.-P. Locquet, J. Perret, J. Fompeyrine, E. Mächler, J. W. Seo, and G. Van Tendeloo, Nature (London) **394**, 453 (1998).
[4] R. Peng, X. P. Shen, X. Xie, H. C. Xu, S. Y. Tan, M. Xia, T. Zhang, H. Y. Cao, X. G. Gong, J. P. Hu, B. P. Xie, and D. L. Feng, Phys. Rev. Lett. **112**, 107001 (2014).
[5] E. J. Monkman, C. Adamo, J. A. Mundy, D. E. Shai, J. W. Harter, D. Shen, B. Burganov, D. A. Muller, D. G. Schlom, and K. M. Shen, Nature Mater. **11**, 855 (2012).
[6] K. Yoshimatsu, K. Horiba, H. Kumigashira, T. Yoshida, A. Fujimori, and M. Oshima, Science **333**, 319 (2011).
[7] Y. J. Chang, L. Moreschini, A. Bostwick, G. A. Gaines, Y. S. Kim, A. L. Walter, B. Freelon, A. Tebano, K. Horn, and E. Rotenberg, Phys. Rev. Lett. **111**, 126401 (2013).
[8] Y. J. Chang, C. H. Kim, S.-H. Phark, Y. S. Kim, J. Yu, and T. W. Noh, Phys. Rev. Lett. **103**, 057201 (2009).
[9] M. Imada, A. Fujimori, and Y. Tokura, Rev. Mod. Phys. **70**, 1039 (1998).
[10] J. Chakhalian, A. J. Millis, and J. Rondinelli, Nature Mater. **11**, 92 (2012).
[11] H. Y. Hwang, Y. Iwasa, M. Kawasaki, B. Keimer, N. Nagaosa, and Y. Tokura, Nature Mater. **11**, 103 (2012).
[12] J. Chaloupka and G. Khaliullin, Phys. Rev. Lett. **100**, 016404 (2008).
[13] P. Hansmann, X. Yang, A. Toschi, G. Khaliullin, O. K. Andersen, and K. Held, Phys. Rev. Lett. **103**, 016401 (2009).
[14] P. Hansmann, A. Toschi, X. Yang, O. K. Andersen, and K. Held, Phys. Rev. B **82**, 235123 (2010).
[15] M. J. Han, X. Wang, C. A. Marianetti, and A. J. Millis, Phys. Rev. Lett. **107**, 206804 (2011).
[16] N. Parragh, G. Sangiovanni, P. Hansmann, S. Hummel, K. Held, and A. Toschi, Phys. Rev. B **88**, 195116 (2013).
[17] J. Son, P. Moetakef, J. M. LeBeau, D. Ouellette, L. Balents, S. J. Allen, and S. Stemmer, Appl. Phys. Lett. **96**, 062114 (2010).
[18] R. Scherwitzl, S. Gariglio, M. Gabay, P. Zubko, M. Gibert, and J.-M. Triscone, Phys. Rev. Lett. **106**, 246403 (2011).
[19] D. P. Kumah, A. S. Disa, J. H. Ngai, H. Chen, A. Malashevich, J. W. Reiner, S. Ismail-Beigi, F. J. Walker, and C. H. Ahn, Adv. Mater. **26**, 1935 (2014).
[20] A. V. Boris, Y. Matiks, E. Benckiser, A. Frano, P. Popovich, V. Hinkov, P. Wochner, M. Castro-Colin, E. Detemple, V. K. Malik, C. Bernhard, T. Prokscha, A. Suter, Z. Salman, E. Morenzoni, G. Cristiani, H.-U. Habermeier, and B. Keimer, Science **332**, 937 (2011).
[21] J. Liu, S. Okamoto, M. van Veenendaal, M. Kareev, B. Gray, P. Ryan, J. W. Freeland, and J. Chakhalian, Phys. Rev. B **83**, 161102 (2011).
[22] A. Frano, E. Schierle, M. W. Haverkort, Y. Lu, M. Wu, S. Blanco-Canosa, U. Nwankwo, A. V. Boris, P. Wochner, G. Cristiani,

H. U. Habermeier, G. Logvenov, V. Hinkov, E. Benckiser, E. Weschke, and B. Keimer, Phys. Rev. Lett. **111**, 106804 (2013).

[23] E. Sakai, M. Tamamitsu, K. Yoshimatsu, S. Okamoto, K. Horiba, M. Oshima, and H. Kumigashira, Phys. Rev. B **87**, 075132 (2013).

[24] P. D. C. King, H. I. Wei, Y. F. Nie, M. Uchida, C. Adamo, S. Zhu, X. He, I. Božović, D. G. Schlom, and K. M. Shen, Nat. Nanotechnol. **9**, 443 (2014).

[25] H. K. Yoo, S. I. Hyun, L. Moreschini, H.-D. Kim, Y. J. Chang, C. H. Sohn, D. W. Jeong, S. Sinn, Y. S. Kim, A. Bostwick, E. Rotenberg, J. H. Shim, and T. W. Noh, Sci. Rep. **5**, 8746 (2015).

[26] N. Hamada, J. Phys. Chem. Solids **54**, 1157 (1993).

[27] R. Eguchi, A. Chainani, M. Taguchi, M. Matsunami, Y. Ishida, K. Horiba, Y. Senba, H. Ohashi, and S. Shin, Phys. Rev. B **79**, 115122 (2009).

[28] See Supplemental Material at http://link.aps.org/supplemental/10.1103/PhysRevB.93.035141 for a clearer presentation of the abrupt electronic-structure changes between four and three UCs by MDC plots.

[29] J. B. Torrance, P. Lacorre, A. I. Nazzal, E. J. Ansaldo, and C. Niedermayer, Phys. Rev. B **45**, 8209 (1992).

[30] P. W. Anderson, Science **235**, 1196 (1987).

[31] X. J. Zhou, P. Bogdanov, S. A. Kellar, T. Noda, H. Eisaki, S. Uchida, Z. Hussain, and Z.-X. Shen, Science **286**, 268 (1999).

[32] S. Raj, T. Sato, S. Souma, T. Takahashi, D. D. Sarma, P. Mahadevan, J. C. Campuzano, M. Greenblatt, and W. H. McCarroll, Phys. Rev. B **77**, 245120 (2008).

[33] T. Giamarchi, *Quantum Physics in One Dimension* (Oxford University Press, Oxford, 2003).

[34] F. D. M. Haldane, J. Phys. C: Solid State Phys. **14**, 2585 (1981).

[35] C. Kim, A. Y. Matsuura, Z.-X. Shen, N. Motoyama, H. Eisaki, S. Uchida, T. Tohyama, and S. Maekawa, Phys. Rev. Lett. **77**, 4054 (1996).

[36] J. W. Allen, G.-H. Gweon, R. Claessen, and K. Matho, J. Phys. Chem. Solids **56**, 1849 (1995).

[37] B. J. Kim, H. Koh, E. Rotenberg, S.-J. Oh, H. Eisaki, N. Motoyama, S. Uchida, T. Tohyama, S. Maekawa, Z.-X. Shen, and C. Kim, Nat. Phys. **2**, 397 (2006).

[38] S. B. Lee, R. Chen, and L. Balents, Phys. Rev. B **84**, 165119 (2011).

[39] J. A. Alonso, J. L. García-Muñoz, M. T. Fernández-Díaz, M. A. G. Aranda, M. J. Martínez-Lope, and M. T. Casais, Phys. Rev. Lett. **82**, 3871 (1999).

[40] M. Medarde, C. Dallera, M. Grioni, B. Delley, F. Vernay, J. Mesot, M. Sikora, J. A. Alonso, and M. J. Martínez-Lope, Phys. Rev. B **80**, 245105 (2009).

[41] J. D. Denlinger, G.-H. Gweon, J. W. Allen, C. G. Olson, J. Marcus, C. Schlenker, and L.-S. Hsu, Phys. Rev. Lett. **82**, 2540 (1999).

[42] G.-H. Gweon, J. W. Allen, and J. D. Denlinger, Phys. Rev. B **68**, 195117 (2003).

[43] D. Mou, R. M. Konik, A. M. Tsvelik, I. Zaliznyak, and X. Zhou, Phys. Rev. B **89**, 201116(R) (2014).

[44] M. Enayat, Z. Sun, U. R. Singh, R. Aluru, S. Schmaus, A. Yaresko, Y. Liu, C. Lin, V. Tsurkan, A. Loidl, J. Deisenhofer, and P. Wahl, Science **345**, 653 (2014).

[45] F. Chen, M. Xu, Q. Q. Ge, Y. Zhang, Z. R. Ye, L. X. Yang, J. Jiang, B. P. Xie, R. C. Che, M. Zhang, A. F. Wang, X. H. Chen, D. W. Shen, J. P. Hu, and D. L. Feng, Phys. Rev. X **1**, 021020 (2011).

[46] E. N. Economou and M. H. Cohen, Phys. Rev. Lett. **25**, 1445 (1970).

[47] P. A. Lee, Rev. Mod. Phys. **57**, 287 (1985).